

## Acoustic Remote Sensing for Irrigation Systems Control in Agriculture

Anna RADIONOVA<sup>1,2</sup>; Chandra Prasad GHIMIRE<sup>3</sup>; Laura GRUNDY<sup>3</sup>; Seth LAURENSEN<sup>3</sup>; Stuart BRADLEY<sup>2,4</sup>; Val SNOW<sup>3</sup>

<sup>1</sup> Department of Physics, The University of Auckland, New Zealand

<sup>2</sup> Auckland UniServices Ltd, New Zealand

<sup>3</sup> AgResearch Ltd, New Zealand

<sup>4</sup> Inverse Acoustics Ltd, New Zealand

### ABSTRACT

The paper addresses the problem of measuring free water on the surface of agricultural soils by an accurate real-time acoustic method. The generation of free water is the result of a fine balance between the irrigation rate and the rate at which the soil can transport water away from the surface and is the primary cause of inefficient and environmentally-harmful losses during an irrigation event. The innovative component of the project is vested in the development of directional acoustic arrays and sophisticated signal processing which can remotely detect free water on the soil surface via changes in reflectivity. The proposed method estimates the amount of free water on the soil surface based on the changes in the amplitude of the reflected sound waves. Our preliminary results show that sound wave reflectivity depends on the proportion of the soil surface covered by water. The presented results are based on both laboratory and field measurements.

Keywords: Acoustic sensor array, Water measurement, Reflected sound wave

### 1. INTRODUCTION

Irrigation provides significant economic benefit to New Zealand and to farmers (1, 2). However, when irrigation transports pollutants (nitrogen, phosphorus, sediment, faecal bacteria and other microorganisms) to water bodies it degrades water quality and so causes significant environmental harm (3-5). A smart technology to improve irrigation by avoiding the transport of pollutants would be transformative for both the industry and the environment. Most of the transport of pollutants occurs when free water is generated on the soil surface (3). Free water is not bound to the soil surfaces but is instead free to flow directly into water bodies, carrying with it pollutants. The conditions on the soil surface that lead to free water vary strongly and unpredictably in space and time and current smart irrigation technology cannot respond to this variation.

Soil is a porous medium with a range of pore sizes and a complex geometry of pores (6-8). The combination of the size range and geometry of the pores opening to the soil surface, slope and micro-topography of the soil surface with the rate at which irrigation is applied determines the development of small isolated pockets of water and then onto the generation of surface water flow (9, 10). The soil surface is naturally rough (9, 11, 12) while the small pockets of water that develop in the surface depressions is smooth. As the proportion of the soil that is covered in water increases, and therefore the risk of runoff also increases, we expect that the acoustic reflectivity of the soil surface will increase.

There is a considerable literature around ground surface acoustic reflectance and absorption properties (13), as a sound wave travels both directly and via reflections from the surface. The semi-empirical models of sound propagation depend on acoustic flow resistivity, and other parameters such as soil porosity. The acoustic flow resistivity is a measure of the air space volume in the soil near the

<sup>1</sup> inverse.acoustics@gmail.com

surface with sound penetration being limited to around 10 mm (14). The near-surface nature of the acoustic interaction is ideal for the purposes of sensing the presence of free water on the soil surface, as water is a more acoustically reflective surface than soil. According to the previous studies, porosity and flow resistivity are considered to be the most important soil characteristics that affect acoustic impedance. The amplitude of the reflected sound wave is expected to increase as the soil becomes more saturated. Rather limited studies can be found in the literature regarding acoustic reflectivity and saturated soil conditions (15-19).

The objectives of this study were to investigate the onset of free water in the soil via changes in reflectivity of the sound waves and to develop an inexpensive and accurate free water sensor for irrigation systems. The preliminary results presented in this paper are based on both laboratory and field measurements.

## 2. THEORETICAL ASPECTS OF THE ACOUSTIC SYSTEM

As described below, we used an acoustic array antenna of length 0.8 m. The ‘far field’ region (Fresnel parameter  $> 1$ ) for this antenna is beyond a range of about 1 m at a frequency of 4 kHz. In our laboratory setup, the distance between the array center to the center of the tray holding the target soil surface is 1.56 m (2.6 array diameters). Thus, the “far field” approximations can be used. The tray subtends an angle of about  $\pm 4^\circ$  at the array.

### 2.1 Phased Array Theory

A linear array of regularly and closely spaced seven KSN1005A super-horn speakers was constructed. This geometry can be described by  $M$  omni-directional speakers having spacing (20):

$$d = D / M \quad (1)$$

where  $D$  is the length of the array, giving a normalised intensity pattern

$$\frac{I(\theta)}{I_0} = \frac{1}{M^2} \frac{\sin^2\left(\frac{1}{2}kD\sin\theta\right)}{\sin^2\left(\frac{1}{2M}kD\sin\theta\right)} \quad (2)$$

where  $k$  is the wavenumber. The KSN1005A speakers are not omnidirectional, but have an angular response, which changes little over the beam-widths. Figure 1 shows the intensity pattern for  $M = 7$ ,  $d = 0.08$  m,  $f = 1$  kHz and 3 kHz, and sound speed  $c = 340$  m s<sup>-1</sup>. The half-power half beam-width is  $c/(2Mfd)$ , or  $17^\circ$  at 1 kHz.

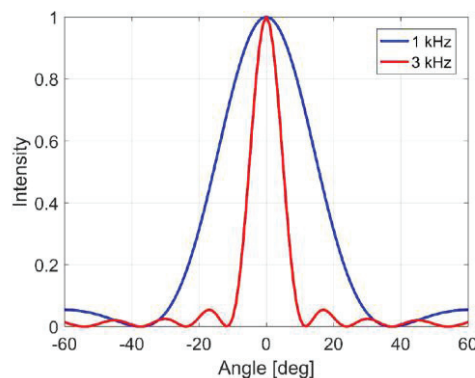


Figure 1 – The theoretical beam pattern for the  $M = 7$  speaker array at frequencies of 1 kHz and 3 kHz

We have evaluated the design in the laboratory environment over the frequency range of 0.5 kHz to 4 kHz in 100 Hz steps, and with time delays between array elements giving peaks shifts of  $0^\circ$ ,  $\pm 30^\circ$ ,  $\pm 45^\circ$ , and  $\pm 60^\circ$ . The angle of sound wave propagation for the phased array can be altered directly from the code. Thirty-six frequencies, seven delays, and measurements at sixteen microphone positions were conducted. One hundred measurements were taken on average for each of these configurations. Figure 2 shows an example of the results for these tests.

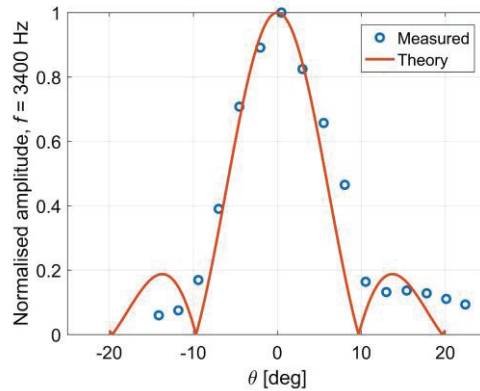


Figure 2 – Measured beam pattern compared with theoretical at 3.4 kHz and a zero progressive time delay between speakers

There are some variations between theory and measurement around the central beam lobe, and larger variations at larger angles. These are most likely due to small variations in speaker gain across the seven speakers. This was optimized by the equalization of the gains for all speakers in the final configuration.

## 2.2 Reflection from Soil and Water

Reflectivity from soil can be estimated by Attenborough's 4-parameter model for the acoustic impedance of a ground surface (21). Typical values of the model's parameters are soil porosity = 0.3, soil tortuosity = 1.35, flow resistivity =  $10 - 10^3$  kPa s m<sup>-2</sup>, and pore shape factor ratio = 0.75. Some results are shown in Figs. 3 and 4, using these values.

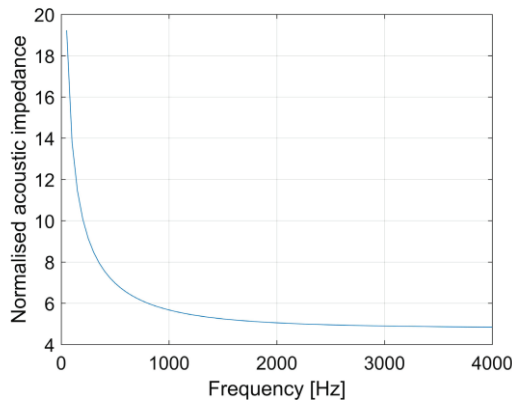


Figure 3 – Normalised acoustic ground impedance as a function of frequency

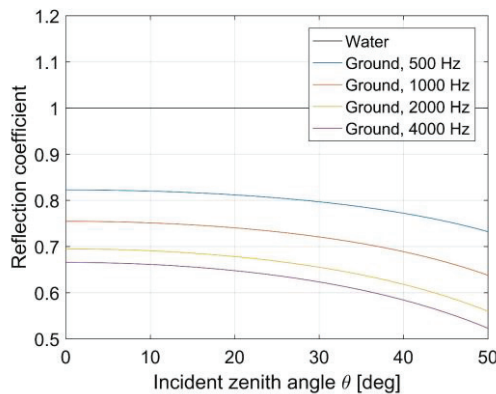


Figure 4 – Reflectivity as a function of incident angle

The greatest frequency variation between water and soil in impedance occurs at low frequencies

(Figure 3). However, the highest contrast between a water surface (which is generally considered to have a reflectivity of 1) and a soil surface is at higher frequencies (Figure 4). Given the generally sharper beam at higher frequencies, and the better soil-water contrast at higher frequencies, the optimum operating frequency for future experiments was selected in a range from 2 to 4 kHz.

### 3. LABORATORY BASED MEASUREMENTS

#### 3.1 Experimental Set Up

The preliminary experiments were designed to determine how different soil water contents affected the amplitude of the acoustic signal. The laboratory set up for these experiments is shown in Figure 5.

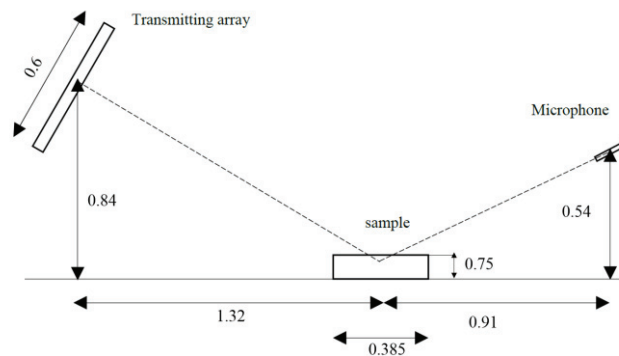


Figure 5 – Layout of the phased array of speakers (at left), the sample tray (center), and the single microphone (right)

The acoustic sensor consists of the phased acoustic transmitting array and an omnidirectional microphone. The sample trays measured 0.385 m by 0.285 m with the height of dry soil being 0.75 m above the laboratory floor. The dry soil mass was 8.4 kg and estimated soil dry bulk density used for these tests was  $1.02 \text{ kg m}^{-3}$ . The signal amplitudes were recorded for a dry soil, and wet soil with 1 L, 2 L of water added to the sample tray and an over saturated soil (3 L of water added) conditions. The latter sample showed free water covering the soil surface. Soil with added water samples were allowed to equilibrate for at least 24 hours under a plastic cover to prevent slow evaporation.

The laboratory experiments were carried out in an anechoic chamber and experimental code to control the acoustic system was created in MATLAB R2015b.

#### 3.2 Results

Initial tests were conducted in order to determine whether there is a change in signal strength when the soil becomes saturated and pooling of surface water begins and to what extent. The definition of ‘saturated’ and ‘pooling’ here is very crude at this stage, and simply refers to the visually observed surface water in a tray. Measurements were conducted on a dry soil, and with 1, 2, and 3 L of water added to the sample tray while the acoustic array angle was locked at  $45^\circ$ . The results of these measurements are shown in Figure 6.

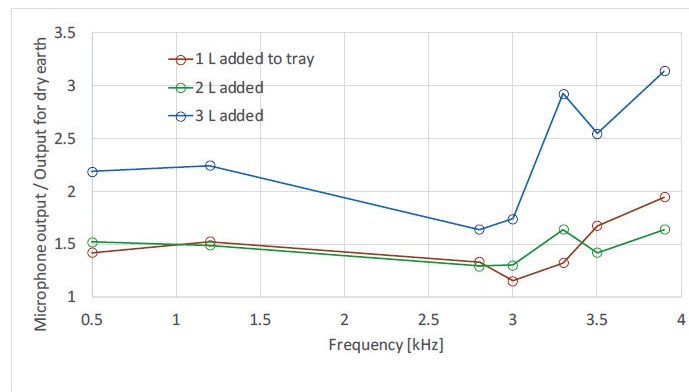


Figure 6 – Normalised (against the relevant dry soil value) microphone output at selected frequencies in the range 0.5 kHz to 3.9 kHz versus water added to the soil sample

Multiple runs were performed over each sample and at each frequency and an averaged result plotted on Figure 6. The errors of these measurements were plotted within the size of data points for each measurement. The 1 and 2 L cases give very similar amplitude reflectivity values. All measurements on wetted soil shows amplitudes around 50% higher than for dry soil measurements and the amplitudes for 3 L added water dramatically increased compared to the 1 and 2 L water added to the dry soil. In addition, these measurements showed that variability increased above a frequency of about 3 kHz. The variability above 3 kHz is most likely due to some direct sound combining destructively and constructively with the reflected sound.

## 4. PRELIMINARY FIELD TESTING OF THE ACOUSTIC SYSTEM

### 4.1 Experimental Set Up

The geometry comprised the speaker array mounted on a tripod and angled at  $45^\circ$  and at the height of the single microphone, which was also on a tripod. Between the two, near the ground, a soil-filled pan with dimensions  $0.6 \times 0.44$  m was placed. This pan was set up a manometer so that water level could be continuously varied. On a frame above these items a downward facing 3D structured light camera (Intel RealSense™ Depth Camera D415) viewed the earth-filled tray, so that its topology could be recorded, including any pooled water. To one side of the array-microphone line a GoPro camera (GoPro Hero 2018) also recorded the surface conditions in the tray (Fig. 7).

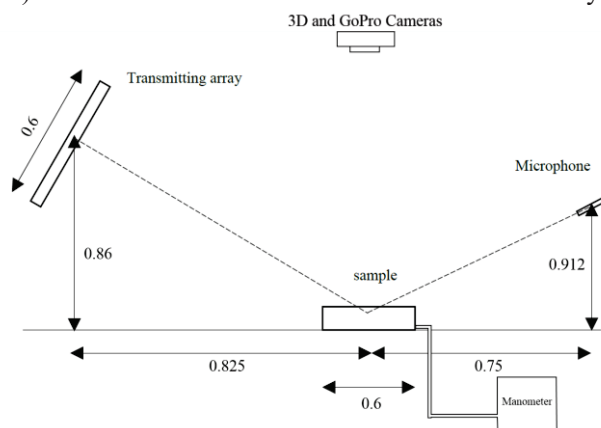


Figure 7 –A schematic diagram of the first field experimental set up with the dimensions.

Sinusoidal pulses of various frequencies and of 10 ms duration were generated and directed toward the soil-filled pan. There are multiple paths to the microphone from each of the seven speakers: directly across the space between speaker and microphone; and bouncing off the soil and surrounding platform and then back upward to the microphone. Acoustic foam placed around the edges of the soil-filled pan helped to reduce the unwanted reflections from the platform.

## 4.2 First Field Experiment Results

In these experiments, all soil samples were initially wet. The “most saturated” example had water ponded on the surface. Figure 8 shows that, over a range of frequencies centred on ~ 3 kHz, there was a clear and consistent demarcation between the ponded water condition and the soil surface condition of wet but not ponded.

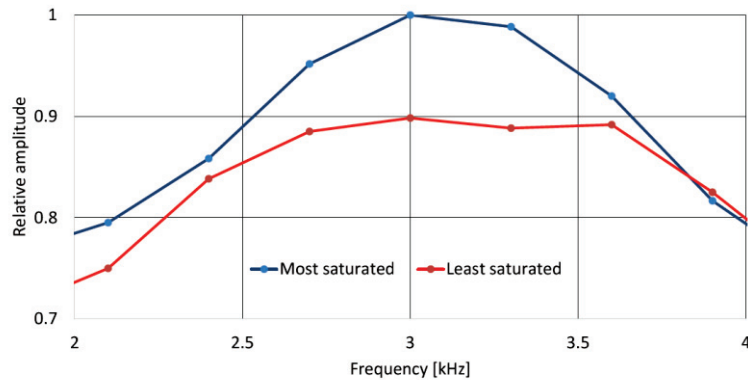


Figure 8 – The relative amplitude of the correlated outputs for a range of frequencies and for a ponded soil surface (blue) and a wet but non-ponded soil surface (red).

The field experiment showed that the basic setup worked outside of the acoustically-controlled laboratory environment. There was a good separation between a soil surface that was merely wet and a surface that was ponded.

## 4.3 Second Field Experiment Results

The acoustic reflectivity experimental procedures during the second field test were carried out in a similar way to the first test. The dimensions and respective distances are indicated in Figure 9. The main difference was in the acoustic signal codes used during this experiment. This time a 13-step Barker code (22) and a two-tone signal were tested on a range of soil conditions in order to increase acoustic sensor performance and tolerance towards environmental sources of noise. Acoustic reflectivity measurements were done for a range of surface wetting conditions (controlled using the manometer), and for frequencies 2.5 kHz – 4.5 kHz with a 0.4 kHz step. Both a tonal pulse, and a 13-step Barker phase-encoded pulse were evaluated. The Barker code was found to give clearer signals.

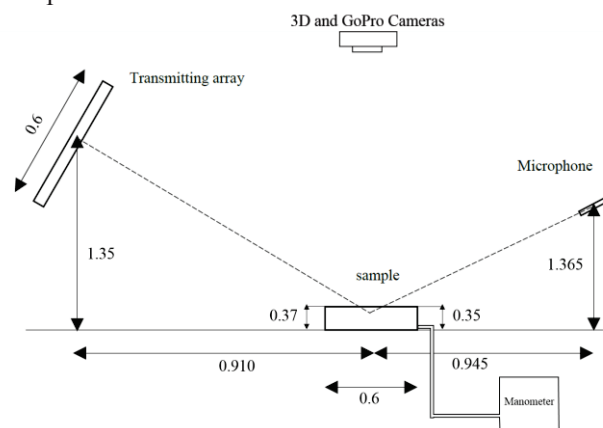


Figure 9 – A schematic diagram of the second field experimental set up with the dimensions.

The 3.3 kHz frequency consistently gave the greatest amplitudes, most likely due to the efficiency of the speakers being high at this frequency (note that the microphone response is flat with frequency). The set up was also tested on a soil sample when it was covered with short grass and it was found grass and its roots in the soil had no clear effect on measured signals during these experiments.

Figures 10 and 11 are characteristic of these results and the errors of these measurements were plotted within the size of data points for each measurement. Figure 10 demonstrates changes of the amplitude of the reflected acoustic signal when soil tray was slowly filled in with water, and shows changes as more and more of the soil surface depressions became filled with water over time. During

this experiment, the measurements were progressively done from dry soil to the state where all the soil surface depressions were connected and filled with water.

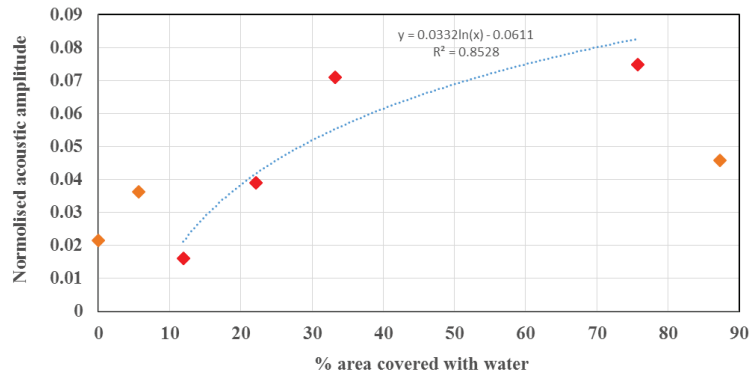


Figure 10 – Normalised amplitude response using a 13-step Barker code for 3.3 kHz (Filling)

Figure 11 shows the reverse process, where initially all the soil surface depressions were connected and filled with water, and at the final stage water was slowly drained from the soil tray over time leaving a wet soil surface.

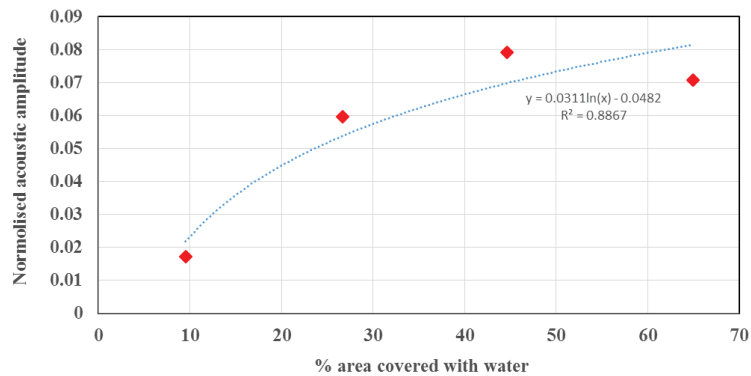


Figure 11 – Normalised amplitude response using a 13-step Barker code for 3.3 kHz (Emptying)

There is a similar variation in measured amplitude at all frequencies. Here the percentage of the tray covered in free water is compared with the normalised acoustic amplitude response. There is a very clear increase in acoustic output up to a free water coverage of 40%, and some indication that the amplitude falls off at very high water coverage. A 13-step Barker code gave best results with respect to signal-to-noise ratios. The trends shown in Figures 10 and 11 are reproducible and similar for both experiments. Figure 11 is lacking the data points for the conditions from 0 to ~ 10% and ~ 90% of soil area covered with water, as during the second experiment, the soil absorbed some water and was wet, while in the first experiment it was initially dry.

## 5. CONCLUSIONS

Preliminary work to develop an acoustic sensor to measure free water on the soil surface was carried out and the sensor system has undergone testing in both laboratory and field environments. Angles from 30° to 60° were tested during the laboratory stage of the sensor development. Based on those results, an angle of 45° was chosen for further testing in the field. The optimal range of frequencies was found to be between 2.5 – 4.5 kHz. This was established over different soil conditions including presence of short grass. Two different acoustic signal codes were tested. It was found that a 13-step Barker code gave better signal-to-noise tolerance compared to more simple tonal signals. The amplitude of the reflected acoustic signal increased with both soil moisture and the proportion of the soil surface covered in water. Our preliminary field results show that the acoustic response is reliable for measurements of the soil surface area covered with water in a range from ~ 10 to ~ 80%, while there are some inconsistencies in acoustic data outside of this range. These inconsistencies might be associated with the prevalence of diffuse components over the specular components in the sound

waves reflected from the soil surface, as these measurements are close to the lower or higher end of different soil conditions. Although the registered signal appeared to be a bit more scattered, it was found that short grass did not significantly adversely affect the measured acoustic signal amplitude.

## ACKNOWLEDGEMENTS

The work reported here was conducted by AgResearch, the University of Auckland and Inverse Acoustics and was funded by New Zealand's Ministry of Business, Innovation and Employment via its Endeavour Fund Smart Ideas contract C10X1708.

## REFERENCES

1. Morgan M, Bidwell V, Bright J, McIndoe I & Robb C. Canterbury strategic water study. Lincoln Environ. Rep. No 4557/1, 2002.
2. Irrigation New Zealand. Socio-economic value of irrigation. Available at: <http://irrigationnz.co.nz/knowledge-resources/irrigation-new-zealand/socio-economic-value-of-irrigation/>. (Accessed: 4th June 2017).
3. McLeod M, Aislabie J, Ryburn J & McGill A. Regionalizing potential for microbial bypass flow through New Zealand soils. *J. Environ. Qual.* 2008; 37.
4. Carter DL. in *Irrigation of Agricultural Crops*. 1990; Agronomy Monograph No. 30: 1143–1171.
5. Blaustein RA, Pachepsky YA, Shelton DR & Hill RL. Release and Removal of Microorganisms from Land-Deposited Animal Waste and Animal Manures: A Review of Data and Models. *J. Environ. Qual.* 2015; 44: 1338.
6. Jure WA, Gardner WR, Gardner WH *Soil Physics* 5th Edition. Wiley and Sons, New York, 1991: pp. 328.
7. Vereecken H. et al. Modeling Soil Processes: Review, Key challenges and New Perspectives. *Vadose Zo. J.* 2016; 15: 1–57.
8. Papanicolaou ATN. et al. Spatial variability of saturated hydraulic conductivity at the hillslope scale: Understanding the role of land management and erosional effect. *Geoderma.* 2015; 243–244: 58–68.
9. Peñuela A, Javaux M, Bielders CL. How do slope and surface roughness affect plot-scale overland flow connectivity? *J. of Hydr.* 2015; 528:192-205.
10. Appels WM, Bogaart PW, van der Zee SEATM. Surface runoff in flat terrain: How field topography and runoff generating processes control hydrological connectivity. *J. of Hydr.* 2016; 534: 493-504.
11. Garcia Moreno R, Diaz Alvarez MC, Saa Requejo A, Valencia Delfa JL & Tarquis AM. Multiscaling analysis of soil roughness variability. *Geoderma.* 2010; 160: 22–30.
12. Xingming Z, Tao J, Xiaofeng L, Yanling D & Kai Z. The temporal variation of farmland soil surface roughness with various initial surface states under natural rainfall conditions. *Soil Tillage Res.* 2017; 170: 147–156.
13. Salomons EM. *Computational atmospheric acoustics*. Springer Science & Business Media. 2001.
14. Taraldsen G & Jonasson H. Aspects of ground effect modeling. *J. Acoust. Soc. Am.* 2011; 129: 47–53.
15. Brandão E, Lenzi A & Paul S. A review of the in situ impedance and sound absorption measurement techniques. *Acta Acust. united with Acust.* 2015; 101: 443–463.
16. Mohamed MHA & Horoshenkov KV. Airborne acoustic method to determine the volumetric water content of unsaturated sands. *J. Geotech. geoenvironmental Eng.* 2009; 135: 1872–1882.
17. Horoshenkov KV & Mohamed MHA. Experimental investigation of the effects of water saturation on the acoustic admittance of sandy soils. *J. Acoust. Soc. Am.* 2006; 120: 1910– 1921.
18. Cramond AJ & Don CG. Effects of moisture content on soil impedance. *J. Acoust. Soc. Am.* 1987; 82: 293–301.
19. Embleton TFW. Tutorial on sound propagation outdoors. *J Acoust Soc Am.* 1996; 100 (1): 31-48.
20. Salomons EM. *Computational atmospheric acoustics*. 2001. Kluwer Academic Publishers. Netherlands.
21. Sabatier JM., Raspert R & Frederickson CK. An improved procedure for the determination of ground parameters using level difference measurements. *J Acoust Soc Am.* 1993; 94 (1): 396-399
22. Adams ER. *Detection and Characterization of Phase-Coded Radar Signals*. Cranfield University (RMCS). UK. 2004. SPC 03-3030.